Moorthy et al., J Theor Comput Sci 2015, 2:4
DOI: 10.4172/2376-130X.1000137

Journal of
Theoretical & Computational Science

Research Article Open Access

Spectroscopic Investigation of the Stimulus of NLO Property on Acetone Thiosemicarbazone Using Computational [HF and DFT] Confinement

Moorthy N[1], Jobe Prabakar PC[1], Ramalingam S[2]*, Periandy S[3] and Pandian GV[4]

[1]Department of Physics, TBML College, Porayar, Tamil Nadu, India
[2]Department of Physics, AVC College, Mayiladuthurai, Tamil Nadu, India
[3]Department of Physics, Tagore Government Arts College, Puducherry, India
[4]Department of Chemistry, TBML College, Porayar, Tamil Nadu, India

Abstract

In this attempt of research work, the inducement of NLO property on the compound Acetone thiosemicarbazone has been analyzed using computational calculations. The FT-IR, FT-Raman, FT-NMR and UV-Visible spectra have been recorded in specified region. The optimized inducement of NLO activity by the molecular structural deformation due to the addition of acetone compound has been investigated. The supportive analyses such as Mulliken charge levels, first order and second order polarization, vibrational confirmation, frontier molecular interactions, thermodynamic function (Gibbs energy) and VCD profile for proving NLO mechanism in the compound have been carried out. The chemical environment of the compound was simultaneously monitored by simulating and recording ^{1}H and ^{13}C NMR spectra. The isotropic and anisotropic chemical shift related to carbons and hydrogens after the formation of target compound have been carefully interpreted. The stabilization of orbitals by interchanging of energy between donor and acceptor was observed by NBO perturbation calculations.

Keywords: Acetone thiosemicarbazone; NLO activity; VCD; Isotropic; NBO perturbation

Introduction

Molecular materials especially, organic materials with nonlinear optical (NLO) properties are presently attracting considerable interest because of their potential applications in the optoelectronic devices of data communications, information storage, optical computing, signal processing [1,2] and terahertz (THz) wave generation [3]. At present, a wide range of stabilized HOMO (Donor) and LUMO (acceptor) substituted organic compounds are being investigated to emphasize the relationship between molecular structure and non linear response. Especially organic structures with large delocalized π-systems are more easily affected by an external optical field as they are relatively loosely bound to the nucleus, and that the delocalized orbitals may be extended over the entire molecule giving large and fast polarization [4,5]. These delocalized π-systems results spatial asymmetry of the electron distribution which is directly associated with Second order NLO-effects [6]. In nonlinear optics, first and second order hyperpolarizabilities are the heart of consideration because of their importance for the production of new materials and devices in opto-electronic industry [7,8].

The thiosemicarbazone is a favored class of compounds of optical chemistry research for recent years because of their crystal structure lacks a centre of symmetry, stability, their optical activity, and their reactivity [9-12]. The thiosemicarbazone and its derivatives are very interesting and have gained special attention in non liner optical application due to their unusual non centro symmetry. As the base compound with potential sulfur and nitrogen donors and hydrogen acceptors, the change in dipole moment and the energy difference between them are causing the second order hyperpolarizability in the compound. Further substitution of CH_3 and other groups in the thiosemicarbazone chain generates functional delocalized π-electron systems such as imine (C=N), thio (C=S) and azine groups (N-N), among which the imine represent a most prominent group. It is interesting to see how the properties change upon this specific subtution of couple of CH_3 fragments as acetone.

After screening the literatures, it was found that, no vibrational and NLO analytical work has been made in the complex system of acetone thiosemicarbazone. In this work, the crystal was fabricated and the important molecular spectra were recorded to evaluate the inducement of optical and NLO properties in the compound. The suitable computational calculations of HF and DFT have been performed and the results obtained in the experimental techniques were evaluated.

Experimental Details

Preparation of acetone thiosemicarbazone

The organic crystal of acetone thiosemicarbazone was prepared by adopting general procedure [13,14]. In a hot solution of thiosemicarbazide, an appropriate amount of methanol was added by drop wise and in the solution of the acetone, measured quantity of methanol during thirty minutes. The mixture was thoroughly stirred and refluxed for four hours. Then, concentrates was filtered half the volume under reduced pressure. The concentrate was allowed for slow evaporation at room temperature. The crystals were collected by filtration and washed with cold ethanol then dried. The grown crystals were purified by repeated- recrystallization.

Spectroscopic measurements of FT-IR, FT-Raman, NMR and UV-Visible spectra

- FT-IR, FT-Raman spectra were recorded in Bruker RFS 27 spectrometer with full specification.

***Corresponding author:** Ramalingam S, Department of Physics, AVC College, Mayiladuthurai, Tamil Nadu, India, Tel: +914364225367; Fax: +914364222264, E-mail: ramalingam.physics@gmail.com

Received November 03, 2015; **Accepted** December 03, 2015; **Published** December 13, 2015

Citation: Moorthy N, Jobe Prabakar PC, Ramalingam S, Periandy S, Pandian GV (2015) Spectroscopic Investigation of the Stimulus of NLO Property on Acetone Thiosemicarbazone Using Computational [HF and DFT] Confinement. J Theor Comput Sci 2: 137. doi:10.4172/2376-130X.1000137

- UV-Visible spectrum was recorded using Lambda 25 Spectrometer with latest specification.
- The ^{1}H and ^{13}C NMR spectral data was obtained from BRUKER 300 FT-NMR spectrometer.

Quantum Chemical Calculations

The calculations of optimization for structural parameters and atomic charges of the title compounds were carried out using the Gaussian 09 D .01 program package [15,16] by using DFT and HF with 6-311++G(d,p) basis set. The optimized parameters were viewed and evaluated from the Gauss view 09 D .01 version [17] and were given in the Table 1. The electronic absorption spectra obtained among the frontier molecular orbitals provides an explanation and estimation of the Kubo gap of the title molecular system and were calculated at B3LYP/6-311++G(d,p) level which exposes the details of chemical reaction path within the molecule. The restricted basis sets are completely described the wave functions in the most popular quantum method in terms of electron density and other properties that were depicted by the possibility of filled NBO. The interaction between bonding and anti-bonding (Rydberg orbitals) signified the divergence of molecular structure from the Lewis model and it was used to measure the delocalization [18,19].

The isotropic and anisotropic chemical shifts in ^{13}C and ^{1}H NMR to explore chemical environment of present compound were simulated in gas and solvent phase (DMSO and chloroform) under GIAO guidance at B3LYP/6-311G++(2d,p) level. Moreover the MEP view has been simulated using B3LYP/6-311++G(d,p) method and their depleted charge levels were represented by specific colors to explore that the reactive sites of the title molecule were evaluated. The thermodynamic functions (the heat capacity, entropy, enthalpy and Gibbs free energy) were calculated for the temperature region 100-1000K from the vibrational wavenumber calculations of the title compound. The VCD spectral analysis has been performed at B3LYP/6-311++G(d,p) level of calculation.

Results and Discussion

Molecular geometry deformation analysis

The present molecular crystal structure; Acetone-thiosemicarbazone fit in to C_S group of symmetry and consists of 17 atoms within the molecule. The compound was made up of thiosemicarbazone chain adopted with couple of methyl group. The methyl groups making Y shape formation on imine group in thiosemicarbazone chain in which the different groups of atoms were found oriented in different planes. The crystal appearance of shaped compound in (111) pane was obtained in the Figure 1. According to the Cartesian coordinate, except methyl hydrogens, the entire molecular group was placed in one plane. In this case, thiosemicarbazone groups of atoms making semi hexagonal ring which causes the asymmetry of charge distribution. Also those groups were making non centro symmetry of the molecule which will lead the molecule fast optical response and was able to self-activate [20].

Two methyl groups on imine group were symmetrically placed in the molecule. But, according to the bond lengths C1-C2 (1.501 Å) and C1-C6 (1.509 Å), C6 group was 0.008 Å stretched out than C1 due to the pulling of N adjacent to the that group. The observed bond length of N10-N11 (1.384 Å) [21] was 0.020 Å greater than calculated value (1.364 Å) due to the C-N charge pulling. Though the imine was loaded on both sides by different group of atoms, there was no change observed in the bond length of C1=N11. This shows that the consistent of the imine group which was the reason for the NLO effect.

Bond Parameters	HF/ 6-311++G(d,p)	B3LYP/ 6-311++G(d,p)	Experimental
Bond Lengths (Å)			
C1-C2	1.502	1.501	-
C1-C6	1.511	1.509	-
C1-N10	1.257	1.284	1.287
C2-H3	1.087	1.095	-
C2-H4	1.081	1.089	-
C2-H5	1.087	1.095	-
C6-H7	1.081	1.089	-
C6-H8	1.086	1.096	-
C6-H9	1.086	1.096	-
N10-N11	1.361	1.364	1.384
N11-H12	0.994	1.012	-
N11-C13	1.344	1.371	1.346
C13-S14	1.683	1.677	1.669
C13-N15	1.328	1.346	1.326
N15-H16	0.991	1.004	-
N15-H17	0.993	1.009	-
Bond Angles (°)			
C2-C1-C6	117.814	118.507	-
C2-C1-N10	117.654	117.474	-
C6-C1-N10	124.531	124.018	-
C1-C2-H3	110.146	110.614	-
C1-C2-H4	110.662	110.70	-
C1-C2-H5	110.146	110.614	-
H3-C2-H4	109.230	108.961	-
H3-C2-H5	107.355	106.890	-
H4-C2-H5	109.230	108.961	-
C1-C6-H7	110.653	111.012	-
C1-C6-H8	110.979	111.336	-
C1-C6-H9	110.979	111.336	-
H7-C6-H8	107.995	107.743	-
H7-C6-H9	107.995	107.743	-
H8-C6-H9	108.115	107.488	-
C1-N10-N11	118.889	118.671	115.1
N10-N11-H12	122.624	123.066	-
N10-N11-C13	121.132	121.227	119.3
H12-N11-C13	116.243	115.706	-
N11-C13-S14	120.133	120.265	119.5
N11-C13-N15	116.540	115.185	117.5
S14-C13-N15	123.326	124.548	122.9
C13-N15-H16	118.077	118.322	-
C13-N15-H17	120.799	120.071	-
H16-N15-H17	121.122	121.605	-
Dihedral Angles (°)			
C6-C1-C2-H3	59.1162	59.1196	-
C6-C1-C2-H4	180.0002	180.0001	-
C6-C1-C2-H5	-59.1157	-59.1194	-
N10-C1-C2-H3	-120.8838	-120.8804	-
N10-C1-C2-H4	0.0003	0.0001	-
N10-C1-C2-H5	120.8843	120.8806	-
C2-C1-C6-H7	-0.004	0.0	-
C2-C1-C6-H8	119.8733	120.0351	-
C2-C1-C6-H9	-119.8818	-120.0351	-
N10-C1-C6-H7	179.996	-180	-
N10-C1-C6-H8	-60.1267	-59.9649	-
N10-C1-C6-H9	60.1182	59.9649	-

C2-C1-N10-N11	-180.0003	-180.0001	-
C6-C1-N10-N11	-0.0002	-0.0001	-
C1-N10-N11-H12	0.0158	-0.0009	-
C1-N10-N11-C13	-180.0046	-180.0001	-
N10-N11-C13-S14	180.0084	-180.001	-
N10-N11-C13-N15	0.0095	-0.0015	-
H12-N11-C13-S14	-0.0108	-0.0002	-
H12-N11-C13-N15	-180.0097	-180.0007	-
N11-C13-N15-H16	179.999	-180.0037	-
N11-C13-N15-H17	-0.0031	0.0038	-
S14-C13-N15-H16	0.0002	-0.0042	-
S14-C13-N15-H17	-180.0019	180.0033	-

Table 1: Optimized bond parameters of Acetone Thiosemicarbazone.

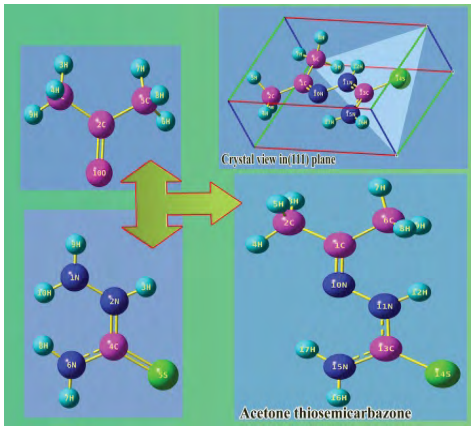

Figure 1: Molecular formation of Acetone thiosemicarbazone.

The observed C-S bond length was 0.008 Å lesser than the calculated value since the increment of the existed force constant. The bond angle C6-C1-N10 was to be the semi ring, but in this case, the methyl loading enhanced the bond angle 124° instead of 120°. The bond angle N10-N11-C13 was 6.04° greater than N11-C13-N15 in the semi hexagonal ring due to the substitution of S atom. This view showed the trouble of the semi hexagonal ring. The bond angle of C13-N15-H17 was exactly 120° which has not affected and making base moiety of the ring.

Mulliken charge distribution analysis

Usually, the design of organic molecular structure with equilibrium of charge distribution for the active response of optical activity is difficult. But, by adding the suitable ligands with the base, the desired charge distribution for the active optical response is easy. In this way, the thiosemicarbazone base was added with acetone and the preferred charge level arrangement was constructed. The thiosemicarbazone chain has specific bond length with imine and amine group of atoms which was fused with methyl twin. The Mulliken charge assignment was presented in the Table 2 and the related diagram was displayed in the Figure 2.

In this present case, the highly positive atoms were represented by green color whereas highly negative atoms red color. Faded red color atoms showed less negative atoms and block color atoms symbolized neutral. Here thiocarbazone group was cemented with acetone molecule, thereby; the imine and azine groups were created in addition with thio group. Generally, in C=S and C=N groups, C and N and S would be positive and negative respectively and make the bond highly dipole character. But here, after the substitution of the CH_3 groups in the compound, the C becomes highly negative and H turns out to be positive and thus the dipole with high degree was made in the methyl groups. Similarly, the N-H bonds become highly dipole. In the case of C=S, the positive level of C reduced much and the dipole character was faded. The Mulliken charge levels were drastically fluctuated in the corner atoms of the compound where as the core atoms were neutralized as much. The dipole moment of the entire compound was bringing out from such corner dipoles. After the substitution of CH_3 group in the compound, the charge levels were redistributed and pulled by them. Except C1, the entire C was negative and N11 was less positive. The atoms in core joint were neutral to produce asymmetry of charge distribution among the atoms of the compound. This was the

Atoms	HF/6-311++G(d,p)	B3LYP/6-311++G(d,p)
1C	0.164291	0.008718
2C	-0.532651	-0.489315
3H	0.148793	0.150688
4H	0.163002	0.16011
5H	0.168023	0.170326
6C	-0.614225	-0.541371
7H	0.15346	0.158284
8H	0.116856	0.115051
9H	0.199714	0.195888
10N	0.050244	-0.030633
11N	-0.02426	0.14684
12H	0.182117	0.147592
13C	-0.002273	-0.195262
14S	-0.449985	-0.31576
15N	-0.275397	-0.18447
16H	0.273727	0.246716
17H	0.278564	0.2566

Table 2: Mulliken atomic charge distribution of Acetone Thiosemicarbazone.

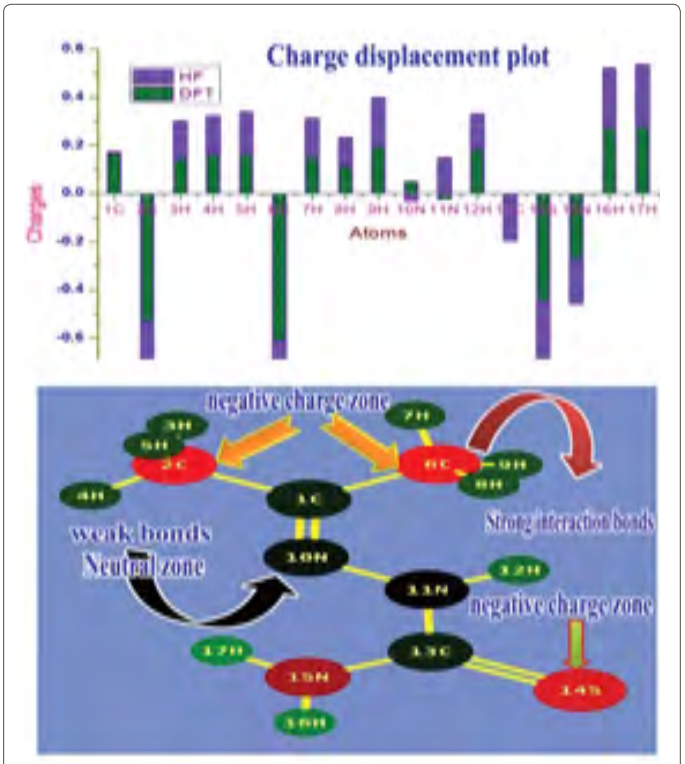

Figure 2: Mulliken Charge Distribution in the compound.

main basis of the present compound to be non centro symmetric and NLO active.

Vibrational assignments

The group frequencies from fundamental wavenumbers of Acetone thiosemicarbazone have been assigned according to their characteristic vibrational regions. The molecule belongs to C_s point group symmetry that contains 17 atoms and it undergoes 45 normal vibrational modes. These active fundamental vibrations were distributed as 31 in plane vibrations denoted by A′ species and 14 out of plane vibrations denoted by A″ species, i.e., $\Gamma_{vib}=31A'+14A''$. The observed FT-IR and FT-Raman frequencies and calculated fundamentals at HF and DFT levels using the triple split valence basis set along with the diffuse and polarization functions; 6-311++G(d,p) have been presented in Table 3. And their respective spectra were displayed in the Figures 3 and 4. Comparison of calculated frequencies with the experimental values reveal the over estimation of the calculated vibrational modes due to the neglect of a harmonicity in real system. Inclusion of electron correlation in the density functional theory to certain extends makes the frequency values smaller in comparison with the HF data.

Methyl group vibrations: In the present case, two methyl groups were present and it was most significant, because they are only the substitutional group in the compound. The fundamental vibrational modes of methyl groups are known to be influenced by the interactions such as electronic effects and intermolecular hydrogen bonding [22]. Electronic effects; back-donation and induction, mainly caused by the presence of C with the chain to CH_3 group, can shift the position of C-H stretching and bending modes [23,24] to the lower region. The

S No	Observed frequencies (cm^{-1})		Calculated frequencies (cm^{-1})		Species	Vibrational assignments
	FT-IR	FT-Raman	HF/6-311++G(d,p)	B3LYP/6-311++G(d,p)		
1	3450vs	3450vs	3411	3445	A′	(N-H)υ
2	-	3400vs	3381	3416	A′	(N-H)υ
3	3240s	3240w	3241	3235	A′	(N-H)υ
4	3000m	3000vs	2990	2991	A′	(C-H)υ
5	2970w	2970s	2979	2983	A′	(C-H)υ
6	-	2960s	2938	2959	A′	(C-H)υ
7	-	2950s	2931	2958	A′	(C-H)υ
8	-	2940s	2933	2938	A′	(C-H)υ
9	-	2920s	2930	2913	A′	(C-H)υ
10	1560vs	1560vs	1565	1562	A′	(C=N)υ
11	1520s	1520vs	1501	1518	A′	(C=S)υ
12	1440m	1440s	1442	1448	A′	(N-H) δ
13	-	1430w	1431	1425	A′	(N-H) δ
14	-	1410w	1406	1404	A′	(N-H) δ
15	-	1340s	1355	1342	A′	(C-N)υ
16	1260s	1260s	1248	1272	A′	(C-N)υ
17	1250w	1250s	1232	1248	A′	(C-C)υ
18	-	1190s	1201	1188	A′	(C-C)υ
19	-	1180s	1198	1182	A′	(N-N)υ
20	1150w	1150m	1146	1146	A′	(C-H) δ
21	1110vs	1110s	1120	1102	A′	(C-H) δ
22	-	1100s	1105	1096	A′	(C-H) δ
23	1070w	-	1069	1068	A′	(C-H) δ
24	-	1050m	1060	1051	A′	(C-H) δ
25	1040w	-	1040	1039	A′	(C-H) δ
26	870s	-	862	866	A"	(N-H) γ
27	-	850s	851	856	A"	(N-H) γ
28	-	840s	845	839	A"	(N-H) γ
29	780s	-	779	777	A"	(C-H) γ
30	-	770s	763	769	A"	(C-H) γ
31	-	760s	750	759	A"	(C-H) γ
32	-	690s	689	681	A"	(C-H) γ
33	-	620m	609	613	A"	(C-H) γ
34	-	610m	610	599	A"	(C-H) γ
35	-	550s	553	545	A′	(C-N) δ
36	-	520m	522	536	A′	(C-N) δ
37	480m	-	483	479	A′	(C=N) δ
38	410w	-	404	413	A′	(C-C) δ
39	340w	-	338	340	A′	(C-C) δ
40	300w	-	300	289	A′	(N-N) δ
41	280w	-	278	284	A"	(C-N) γ
42	240w	-	247	230	A"	(C-N) γ
43	210w	-	212	210	A"	(C-C) γ
44	180w	-	184	174	A"	(C-C) γ
45	110w	-	108	104	A"	(N-N) γ

Table 3: FT-IR and FT-Raman experimental and calculated (scaled) vibrational frequencies of Acetone Thiosemicarbazone.

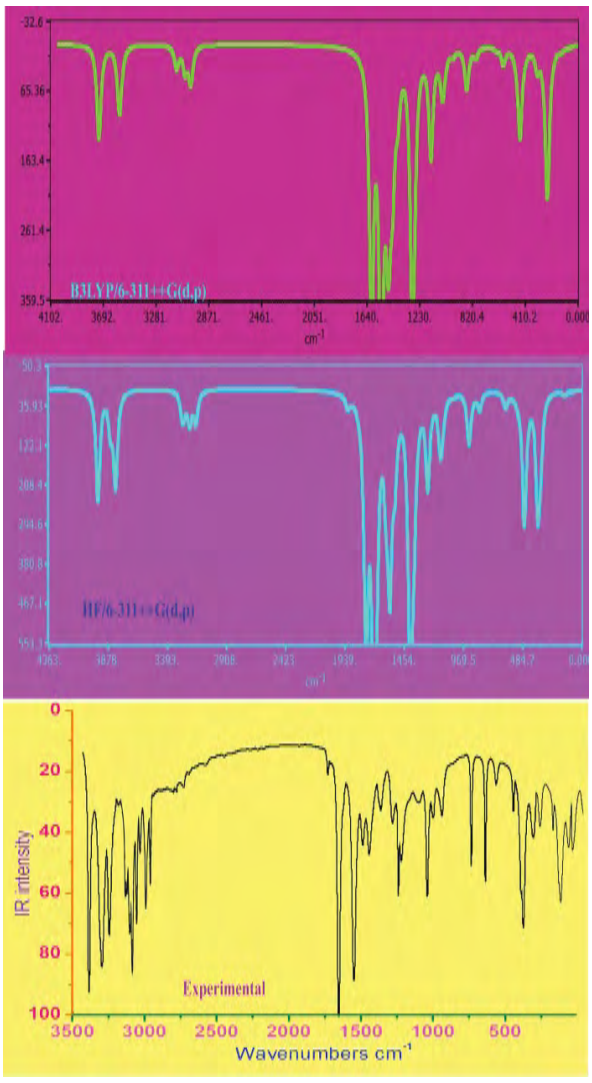

Figure 3: Experimental and calculated FT-IR spectra of Acetone Thiosemicarbazone.

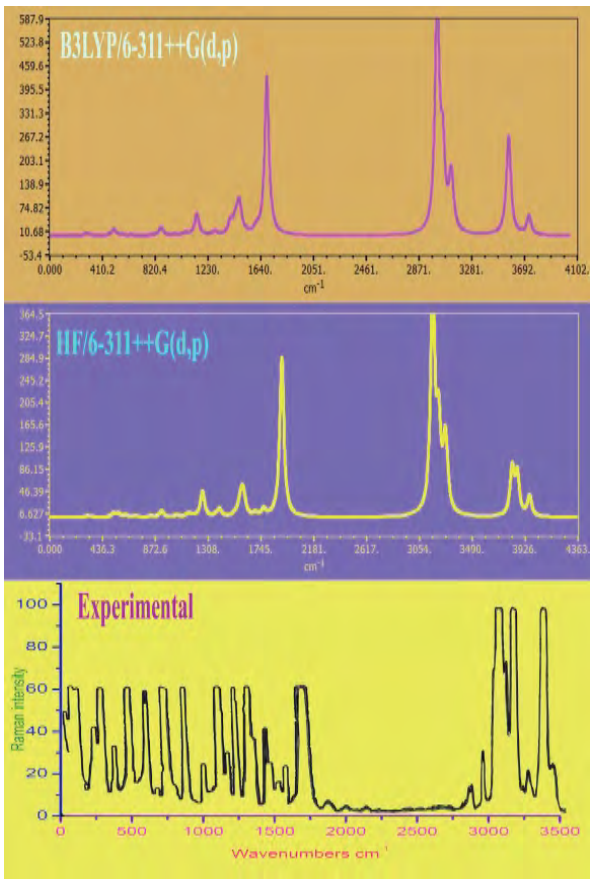

Figure 4: Experimental and calculated FT-Raman spectra of Acetone Thiosemicarbazone.

assignments of methyl group vibration make a significant contribution to the title molecule since it controls all other vibrations. The presence of C-H vibrations emphasized that, the place of methyl group in the chain. In CH_3 substituted compounds, the C-H asymmetric and symmetric stretching vibrations appear in the range 2975-2840 cm^{-1} and 2870-2825 cm^{-1} respectively [25]. In the present case, the IR and Raman bands were at 3000, 2970, 2960, 2950, 2940 and 2920 cm^{-1} assigned to asymmetric C-H stretching vibrations. Though C-H was pure dipole bond, most of the bands were appeared in Raman spectrum instead of IR. These vibrational bands ensured the strong polarization existed in the compound. All these bands were observed at the top of the expected region which is due to the dominance character.

The C-H in-plane and out-of-plane bending vibrations for methyl substituted compounds are observed in the region of 1250-900 cm^{-1} and 650-900 cm^{-1} respectively [26-28]. Here, the C-H in-plane bending peaks were observed at 1150, 1110, 1100, 1070, 1050 and 1040 cm^{-1} and the out-of-plane bending vibrations identified at 780, 770, 760, 690, 620 and 610 cm^{-1} respectively. According to the reported literature [29,30], the entire in plane bending modes were found within the expected region whereas two of out of plane bending peaks were moved little behind the characteristic region. Hence, from this observation, it was clear that, this state of enhancement of CH_3 vibrations in the vibrational pattern of the present compound ensured the existence of its physical and chemical property in the thiosemicarbazone.

N-H vibrations: Generally, N-H bonds in amine group always placed a consistent place in the entire vibrational pattern of the IR and Raman spectra due to their rich force constant. This is the uniqueness of the amine group which is usually dominates entire vibrational motion o the compound. Here, three N-H bonds acknowledged with the thiosemicarbazone group in the compound. The N-H bonds have to produce 9 vibrational modes and it will be the part of the whole vibrational pattern. Frequently, hetero nuclear bond N-H show its stretching vibration in the region 3500-3150 cm^{-1} [31]. The place of IR absorption of N-H vibration in the region depends upon the nature of hydrogen bonding and the substitutional effect [32]. In the present compound, thiosemicarbazone reserved three N-H bonds and the consequential stretching vibrations were found with very strong intensity in IR and Raman at 3450, 3400 and 3240 cm^{-1}. The observed N-H stretching vibrations have not affected and also out of three vibrations, all were identified asymmetric. In this compound, except amino group, there were no dominated vibrations found. These stretching vibrations generally have not disturbed and this is true in this case.

The N-H bending (scissoring) vibrations usually observed in the region 1580-1640 cm^{-1} and the rocking modes are assigned in the range 1170-1080 cm^{-1} in thio amides which may be affected slightly by the inductive effect with high electronegative group [33-35]. Here, three in plane bending modes observed at 1440, 1430 and 1410 cm^{-1}. Here, these vibrational modes should not be the scissoring bands since; the dominating vibrational bands should not be affected much. So, those bands were to be the rocking modes that were found encouraged above the expected region. This was mainly due to the thio group present in the compound which was also the root cause of the optical properties. The out of plane bending vibrations in thio amides are observed in the region 710-580 cm^{-1} [36]. Accordingly, the out of plane bending modes were identified at 870, 850 and 840 cm^{-1}. Similar to the in plane bending, all the out of plane bands were elevated and prove its leading character. The source of second order optical response in crystal lattice was thio amide group and it was progressive in this compound.

C=N, C-N and N-N vibrations: The significant dipole bond (C=N and C-N) which was existed along with azine due to the substitution of methyl groups in the compound. Generally, the C=N stretching vibration has high force constant (13.43 mDyne/A) and high Raman activity (392.32 A^4/AMU) observed in the region 1600-1490 cm^{-1} [37]. In this case, the vibrational band was found with very strong intensity at 1560 cm^{-1} in IR and Raman. This strong symptom of appearance the imine group ensured its very active presence. It's in plane bending was present at 480 cm^{-1} which was also ensured the activity extension. Another important existence of dipole bond C-N and the resultant stretching absorption peak were observed in the region 1382–1266 cm^{-1} for amine derivatives [38]. In amide compound, the band observed at 1368 cm^{-1} was assigned to be due to C–N stretching [39]. Hence, in this case, two strong bands were observed at 1340 and 1260 cm^{-1} for C-N stretching vibrations. The in plane and out of plane bending vibrations are found at 550 and 520 cm^{-1} and 280 and 240 cm^{-1}. The stretching vibrations have not affected whereas entire bending vibrations have suffered much due to the azine and thio group.

The rare electron-electron interaction bond N-N which is important core bond of azine group since it was bridge point for creating active NLO properties for title compound. Normally, the azine bond N-N stretching vibration was observed around 1080 cm^{-1} [40]. The N-N stretching vibration was strongly found at 1180 cm^{-1} in Raman spectrum only. This shows the higher optical activity of the molecule. The following in plane and out of plane bending modes was observed at 300 and 110 cm^{-1} respectively. The obtained azine group peaks were

precisely harmonized with the literature and confirm its presence and explored the optical-semiconducting properties of the compound.

NMR profile: Nuclear magnetic resonance (NMR) spectroscopy has evolved as one of the most powerful analytical techniques for evaluating chemical properties of the organic compound. It permits to visualize single atoms and molecules in various media in solution as well as in solid state. NMR is nondestructive and gives molar response that allows structure elucidation and quantification simultaneously. The information provided by NMR spectroscopy regarding the structure of compounds has made this technique a great tool for the identification and characterization of base and ligand groups. When compared to other analytical techniques, NMR spectroscopy is one of the least sensitive techniques [41]. In this case, the optimized structure of present molecule is used to calculate the NMR spectra at B3LYP method with 6-311++G(d,p) level supported by GIAO method and the chemical shifts of the compound are reported in ppm relative to TMS for ^{1}H and ^{13}C NMR spectra which were presented in Table 4 and the corresponding spectra were shown in Figure 5.

The NMR signals are usually separated into different domain of peaks with respect the diamagnetic equivalence of carbon and hydrogen atoms. In this case, the carbons were appeared in three dissimilar environments such as methyl C, amine C and imine C. The chemical shift of C13 was more shifted than C1, C2 and C6 since its shield was completely broken by the loading of N and S atoms unevenly. The observed isotropic chemical shift of C1 was 141 ppm and it was high when compared with C2 and C6. This was mainly due to the breaking of paramagnetic shield by methyl and imine groups. The chemical shift of C2 and C6 were very low and below 50 ppm which was due to the further shielding of delocalized electrons. It was also evidenced (negative carbons) in the Mulliken charge analysis. The chemical shift of hydrogens in amine group was high when compared with methyl hydrogens which was mainly due to the coupling of N. The chemical shift of methyl hydrogens found to be very low due to the highly positive flavor occurrence. The entire hydrogen atoms in this compound were found with high degree of positive flavor which was due to making intensive dipole with corresponding atoms. Thus, entire

Atom	^{1}H NMR				Atom	^{13}C NMR			
	Experimental	Theoretical (B3LYP)				Experimental	Theoretical (B3LYP)		
		Gas	DMSO	Chloroform			Gas	DMSO	Chloroform
H12	9.9	7.82	7.98	7.93	**C13**	181	185.8	184.68	185.18
H17	8.6	6.58	7.03	6.90	**C1**	151	146.96	157.34	154.52
H16	7.9	5.41	5.71	5.63	**C2**	40.3	26.45	26.63	26.58
H5	4.5	1.98	2.17	2.11	**C6**	17.6	13.88	14.41	14.24
H3	3.3	1.98	2.17	2.11	-	-	-	-	-
H4	2.5	1.81	1.77	1.79	-	-	-	-	-
H8	1.9	1.72	1.84	1.81	-	-	-	-	-
H9	1.8	1.72	1.84	1.81	-	-	-	-	-
H7	1.8	1.64	1.88	1.81	-	-	-	-	-

Table 4: Experimental and calculated ^{1}H and ^{13}C NMR spectral data of Acetone Thiosemicarbazone.

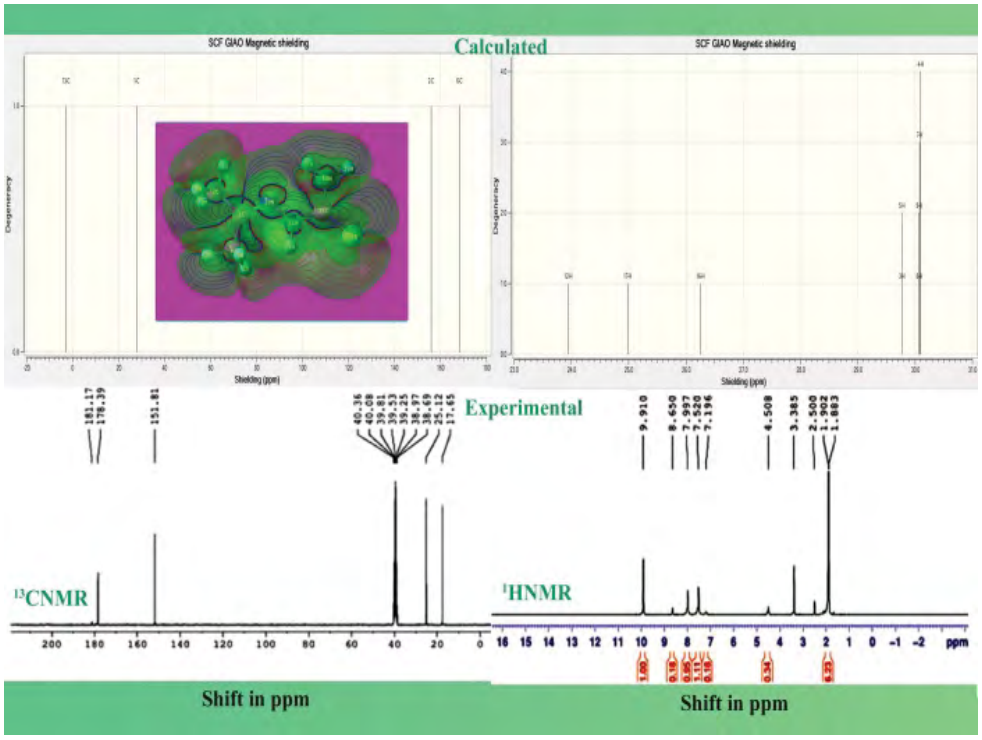

Figure 5: Experimental and simulated ^{13}C and ^{1}H NMR spectra of Acetone Thiosemicarbazone.

hydrogens in the compound were participated in the alternation of the chemical properties of the compound.

Frontier molecular analysis- electronic properties: The frontier molecular orbitals are very much useful for studying the electric, linear and non linear optical properties of the organic compound. The stabilization of the molecular- bonding orbital and destabilization of the antibonding orbital is achieved by the overlapping of two orbitals [42]. In the case of molecular orbital interaction, two important molecular orbitals called frontier orbitals (HOMO and LUMO) interact with each other. After the formation of molecular orbital, generally, the electron density will occupy at the region between two nuclei. In the molecular orbital, the in-phase interaction (bonding orbital) and out of phase interaction (anti bonding molecular orbital) is taking place in ligand and base molecule [43].

The 3D diagram of the frontier molecular orbitals, HOMO and LUMO for title compound were displayed in Figure 6. From the figure, it was noted that, the HOMO was mainly localized over the π-orbital lobe of carbon and sulphur coupling of thio group and the region upon which the electron cloud with intense density that was common for both C and S. from this condition, it was inferred that, the thio group acting as donor for N-H, C-N bonding interaction. The σ-bond lobe interactions were identified N-N, C-N and N-H bonds which also acted as donor for the interaction. There was spatial extension formed up in the C=S π-delocalization. In LUMO, there were so many empty interactive orbitals appeared in S, C-N, C-C, C-H, N-N and N-H which were able to create σ-orbital lobe interactions. The σ-bonding interactions were identified in different bonds of LUMO and also some of the extreme cascade orbital interactions appeared in the core bonds. The σ- electrons interactions taking place in between thio group (donor) and methyl groups (acceptor) in which several lobe were interacted with one another and making as chain orbitals. This was the main reason for the reducing the energy gap of the compound. The calculated electronic energy gap was found to be 3.54 eV which was in the range of semiconducting property. In addition to that, in the case of subsequent orbitals in LUMO-1, the σ-bond lobe interaction was made together to form umbrella shape spatial quantization of orbitals and it was clearly seen in the Figure 6.

Optical properties analysis: Generally, UV/Vis spectroscopic tool is used in analytical chemistry for the quantitative determination of different bonded elements, such as highly conjugated molecular system in base compound. UV-Visible spectroscopy is useful in the structure elucidation of organic molecules related to chromophores and to study the optical property the molecule and also to detect the NLO activity of the compound. The calculations of the electronic structure and electronic energy excitation were calculated at the B3LYP/6-311++G(d,p) level using the TD-DFT approach in gas phase and with the solvent of DMSO and Chloroform. The calculated excitation energies, oscillator strength (*f*) and wavelength (λ) and spectral assignments are given in Table 5. The TD-DFT calculations predicted that, irrespective of the gas and solvent phase, the entire transitions belong to quartz ultraviolet region. In the case of gas phase, the strong transition was observed at 254.58 nm with maximum oscillator strength f=0.23 with 4.87 eV energy gap. The entire transitions were assigned to n→σ* and n→π*. The designation of the band was R (German, radikalartig) and attributed to the chromophores groups, such as C=N, C=S and N-N group. The electronic transitions belong to hypsochromic shift and the solvent effect was found to be less in this compound. The Frontier molecular orbital interaction in UV-Visible region was depicted in the Figure 7. According to the figure, the σ and π-bond delocalization taken part in the interaction which had given the stabilized energy gap 4.94 eV. This was so high and enough to strong stabilization between optical donor and optical acceptor of the compound. When the LUMO moved to very lower levels, the umbrella molecular interaction was observed which helped to stimulate optical polarization. The experimental UV-Visible spectrum was found to be same as calculated spectrum which was presented in the Figure 8.

In UV-Visible spectra, entire transitions belong to the quarts ultraviolet region (240-340 nm). So the compound also can be used for quarts optics [44]. The consistent peak was observed at 300 nm in both experimental and calculated spectrum which was due to the presence of two π conjugated system of bonds (C=N, C=S) in the compound. From this observation, it was clear that, the present compound is able to produce the optical energy with second and third fold frequency. When it was going from gas to solvent phase, it was determined that, the wavelength region was decreased and simultaneously the energy of the absorption was increased. This was the important evidence of increment of frequency in the present compound.

Molecular electrostatic potential (MEP) maps: The Molecular electrostatic potential view is simulated by the B3LYP/6-311+G(d,p) level of theory and was presented in the Figure 9. The MEP is highly informative concerning the protonic and electronic charge distribution of a given molecule. It is mainly used for biological interactions analysis

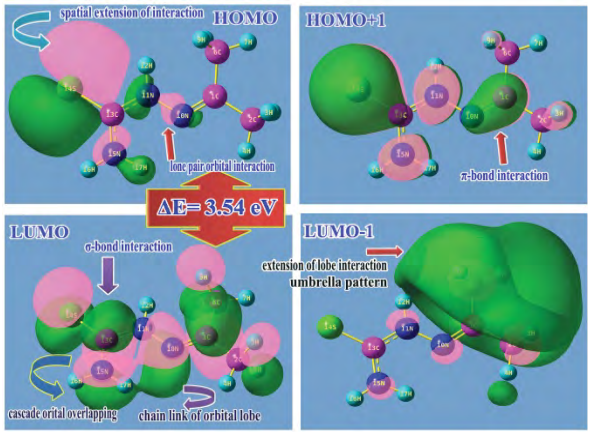

Figure 6: Frontier molecular orbital in IR region.

λ (nm)	E (eV)	(*f*)	Major contribution	Assignment	Region	Bands
Gas						
340.5	3.64	0.0056	H→L (91%)	n→σ*	Quartz UV	R-band (German, radikalartig)
254.5	4.87	0.2301	H-1→L (81%)	n→π*		
244.3	5.07	0.0363	H→L+1 (88%)	n→π*		
DMSO						
334.1	3.71	0.0126	H→L (83%)	n→σ*	Quartz UV	R-band (German, radikalartig)
264.3	4.69	0.3054	H-1→L (79%)	n→π*		
238.8	5.19	0.0141	H-2L (57%), H-3→L (40%)	n→π*		
Chloroform						
336.1	3.69	0.0111	H→L (86%)	n→σ*	Quartz UV	R-band (German, radikalartig)
262.9	4.72	0.3169	H-1→L (82%)	n→π*		
236.3	5.25	0.0117	H-3→L (48%), H-2→L (47%)	n→π*		

Table 5: Theoretical electronic absorption spectra of Acetone Thiosemicarbazone using TD-DFT/B3LYP/6-311++G(d,p) method.

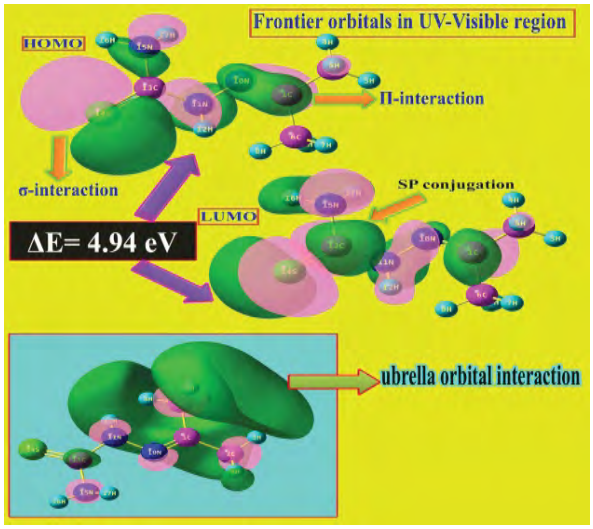

Figure 7: Frontier molecular orbital in UV-Visible region.

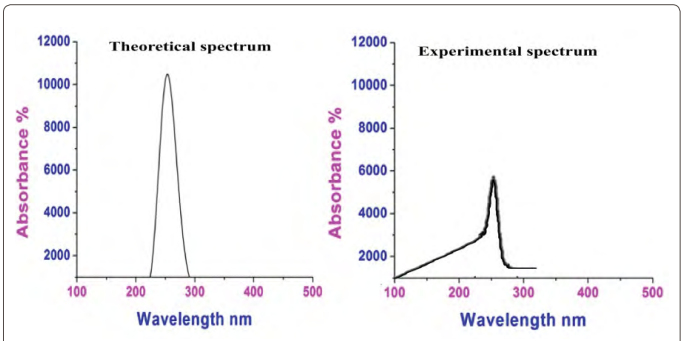

Figure 8: UV-Visible spectra of Acetone Thiosemicarbazone.

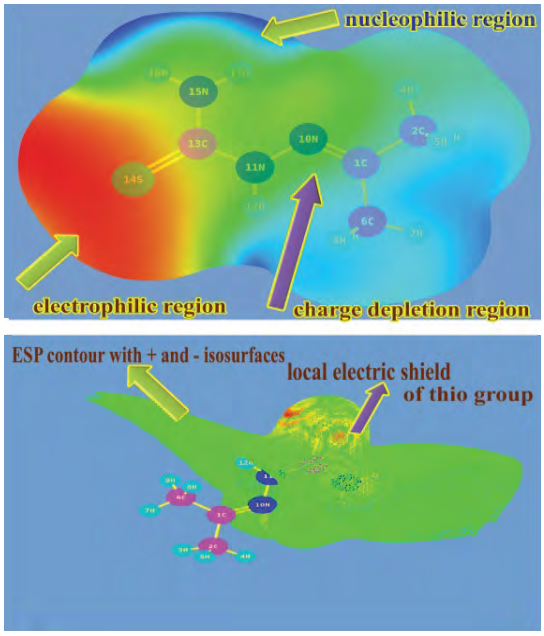

Figure 9: MEP display of Acetone Thiosemicarbazone.

similar to the crystalline state. It is also used for topographical analysis of the electronic structure and molecular reactivity pattern of the complex molecules.

The organic structure with large delocalized π-systems have proven to be more easily affected by an external optical field as they are relatively loosely bound to the nucleus and that the delocalized orbitals may be extended over the entire molecule giving large and fast polarization [45]. The color code of these maps was represented between -6.75 a.u. (genuine red) to 6.75 a.u. (genuine blue). Generally, the negative regions are mainly localized over the portion of highly electronegative atoms. The Figure 9 showed the two extremities of polarized charges in which, the nucleophilic region was appeared wherever the hydrogens present in the compound whereas the electrophilic region was found only on sulphur of thio group. The charge depletion region was identified at the core bonds of the compound. The possibility of the charge separation was taking place strongly between thio and CH_3 groups. This was making resultant strong dipole arrangement in this present compound which will help to the improvement of NLO activity.

NLO activity analysis: To design of efficient NLO compound, in order to increase the nonlinearity, it was important that, the donor acceptor capability in the base compound is to be increased by the substitutions attached to the π-conjugated system. The position of the substitutions is of vital important in terms of NLO activity. The large value of the first hyperpolarizability, which is the measure of the nonlinear optical activity of the molecular system, is associated with intramolecular charge transfer resulting from an electron cloud movement through a π conjugated framework from electron donor to electron acceptor groups.

In this case, the acetone as functional group was added with thiosemicarbazide base, the present compound was capitulated. The calculated parameters were presented in the Table 6. The polarizability (α) and hyper polarizability (β_0) of the thiosemicarbazide were 63 × 10^{-33} esu and 142 × 10^{-33} esu respectively whereas the same for acetone were 40 × 10^{-33} esu and 91 × 10^{-33} esu respectively. But the polarizability (α) and hyper polarizability (β_0) of the present compound were 160 × 10^{-33} esu and 285 × 10^{-33} esu. From this observation it was clear that, the second order and third polarization were streamlined. Thus, the substitutional effect of acetone has extensively improved the non-linearity flavor of the thiosemicarbazone. In addition to that, the position of CH_3 making Y shape structure and was of vital important in terms of NLO activity. The stabilization of the energy between HOMO and LUMO is depends upon the polarization existed in the compound while it absorb the electrical field. This can be identified by measuring the dipole moment. If the compound possesses high degree of dipole moment, normally, the compound will be responding effectively for the flow of local electric field and suppress the wavelength and multiply the frequency. Here, the dipole moment was found to be 5.71 Debye and it was high enough to induce non-linear characteristics.

NBO profile: The natural bond orbital (NBO) calculations were made on natural bonding and antibonding orbital transitions. The calculations has been performed along with the frequency calculation using Gaussian NBO 6.0 program [46] with B3LYP/6-311++G(d,p) method, in order to determine electronic transitions from the filled orbital of one bond system and unfilled antibonding orbital of another system. The NBO profile of the compound was used for the quantity of energy transition, type of delocalization of electron density and kind of hyper conjugation of electronic orbitals. The NBO analysis granted the information regarding electronic orientations inside the molecule

Parameters	B3LYP/6-311++G (d,p)		
μ_x	5.574		
μ_y	1.255		
μ_z	-0.0001		
μ	5.71 (Debye)		
Δα	220.39		
α_{Total}	160.72		
β_{xxx}	61.905		
β_{xxy}	15.499		
β_{xyy}	-2.259		
β_{yyy}	18.994		
β_{xxz}	-0.0003		
β_{xyz}	0.0006		
β_{yyz}	-0.0007		
β_{xzz}	7.112		
β_{yzz}	-0.471		
β_{zzz}	0.0000		
β_{total}	285.718 × 10^{-33} (esu)		
Parameters	**Acetone**	**Thiosemicarbazide**	**Acetone thiosemicarbazone**
Dipole moment (μ) (Debye)	2.9664	4.0548	5.713
Average Polarizabilities (α_0)	64.206	59.652	220.393
Exact polarizability (Δα) × 10^{-33} esu	40.753	63.016	160.727
Hyperpolarizability (β_0) × 10^{-33} esu	91.329	142.517	285.718

Table 6: Calculated electric dipole moments μ (Debye), dipole moment components, α and β_{tot} components of Acetone thiosemicarbazone.

after the renovation of molecular orbitals after the optimized structure was formed.

The Natural Bond Orbitals parameters; occupancy, the energy difference between donors and acceptors, stabilization energy, polarization energy etc, were listed in Table 7. The allowed transitions between various possible donors and acceptors in molecule with their occupancy value were presented in detail. According to the selection rule, the stabilization energy for these transitions gives a measure of the likelihood of these transitions which indicate the highly probable in this molecule. The transition was observed from C1–N10 to N11–C13 (σ–σ* with 10.54 Kcal/mol). This transition indicated that, the energy was transferred between the consecutive bonds of the chain. The transition taking place from C1–N10 to C6-H8 (π-σ*, 10.42 Kcal/mol) which showed that, the energy transformation from hyper conjugation to single electron conjugation system. The exchange of energy was from N10-N11 to C1-C2 and C13-S14 (σ -σ*, 14.4 and 9.6 Kcal/mol) which was to be the important energy transfer since the N-N bond is the vital responsibility for NLO property of the compound.

The N11-C13 to C1-N10 and N15-H16 (σ-σ*, 7.5 and 9.2 Kcal/mol) which showed the maximum possibility of energy exchange and causing the pathway of lobe interaction. This was evidenced in HOMO LUMO energy operation. The energy switching was taking place even from LP N10 to C1-C2 and C1-C6 (σ-σ* with 7.4 and 46.4 Kcal/mol). This transition was rare and found in this compound which tells the strong stabilization arranged in those orbitals. These transitions with high magnitude showed the energy stabilization of the chain. Some of the σ-σ* transitions were taking place between base and substitutions which indicated that, the strong interaction were occurred and leaded to the enhancing of NLO properties of substitutions with the thiosemicarbazone.

Thermodynamical functions analysis: The thermodynamic functions; entropy, specific heat capacity and enthalpy of the crystal compound play a significant process in physical as well as chemical properties. The thermodynamical calculation was performed using NIST program with suitable method; B3LYP/6-311++G (d,p) and was represented in the Table 8 and the corresponding diagram was depicted in the Figure 10. The coefficients of entropy, specific heat capacity and enthalpy are always varied with respect to temperature positively in the case of semiconducting compound. In this case, when the temperature increased from 100K to 1000K, the thermodynamical functions found to vary as linear curve and sustained up to the maximum temperature. This linear variation shows the present compound was being semiconductor.

Similarly, the Gibbs free energy is positive temperature coefficient as well. This positive temperature coefficient of the compound proved to be the optical semiconductor. Normally, the chemical reaction is feasibly occurring when the Gibbs free energy of the molecular system decreases as much as possible. Here, the Gibbs free energy ΔG was found to be negative which revealed that, the chemical reaction was constant and it was inferred that, the present compound was chemically strong and active. The thermodynamic functions are normally reflect the chemical viability of the compound and showed the ability to bind with another ligand groups in order to extend their optical property. Here, the variation of those functions exposed that; the optical property can be tuned further by suitable substituents.

Chemical properties: The physical property of the organic compound is directly related with chemical property. So, the physical parameters are very important to clarify the chemical behavior of the compound. Accordingly, the chemical hardness and potential, electronegativity and Electrophilicity index were calculated and presented in Table 9. Molecules with polar covalent bonds can result in molecules with overall polar attributes. The measure of the overall polarity of a molecule is called the dipole moment. As the value of the dipole moment increases, so does the polarity of the molecule. In this case, the dipole moment reflects linear as well as non linear optical property of the compound which is the capability of electrical and optical polarization of a compound. The large dipole moment leads the compound; very strong intermolecular interactions. The calculated dipole moment value for the present compound was 5.71 Debye and it was comparatively very high enough to induce strong intermolecular interactions. This strong interactive force is able to create second order polarization in the compound.

The chemical hardness is a significant factor which was used to estimate the crystal hardness and thermodynamic stability of organic compound. The chemical hardness was found to be 1.772 which was perceptible magnitude by which the present compound has definite hardness. Here, hardness character was enriched by adding thiosemicarbazone with acetone group. The tendency for an atom to attract electrons is its electronegativity. Usually, the rate of electronegativity is depends upon the functional groups of the compound. Here, the compound was composed by two separate groups of atoms and electronegativity was found to be 6.470, it was relatively high and local polarization was effectively present. Also the property of chemical bonds of title molecule was being ionic.

Type	Donor (i)	Occupancy ED/e	Acceptor (j)	ED/e	E(2) KJ/mol	E(2) kcal/mol	Energy difference E(j)-E(i) a.u.	Polarized energy F(i,j) a.u.
σ -σ*	C1 - C2	1.97808	C1 - N10	0.01912	7.32	1.75	1.25	0.04
			N10 - N11	0.03491	24.81	5.93	1.01	0.07
σ -σ*	C1 - C6	1.98765	C1 - N10	0.01912	5.77	1.38	1.27	0.04
σ -σ*	C1 - N10	1.98856	C1 - C2	0.01904	4.77	1.14	1.33	0.04
			C1 - C6	0.03486	4.94	1.18	1.31	0.04
			N11 - C13	0.0586	10.54	2.52	1.35	0.05
π -σ*	C1 - N10	1.95195	C2 - H3	0.01018	10.42	2.49	0.73	0.04
			C2 - H5	0.01018	10.42	2.49	0.73	0.04
			C6 - H8	0.00908	7.7	1.84	0.72	0.03
			C6 - H9	0.00908	7.7	1.84	0.72	0.03
σ -σ*	C2 - H3	1.97476	C1 - N10	0.01912	7.11	1.7	1.12	0.04
			C1 - N10	0.18809	18.07	4.32	0.53	0.04
σ -σ*	C2 - H4	1.98763	C1 - C6	0.03486	19.2	4.59	0.91	0.06
σ -σ*	C2 - H5	1.97476	C1 - N10	0.01912	7.11	1.7	1.12	0.04
			C1 - N10	0.18809	18.07	4.32	0.53	0.04
σ -σ*	C6 - H7	1.98763	C1 - N10	0.01912	22.43	5.36	1.13	0.07
σ -σ*	C6 - H8	1.97596	C1 - C2	0.01904	7.91	1.89	0.94	0.04
			C1 - N10	0.18809	17.32	4.14	0.54	0.04
σ -σ*	C6 - H9	1.97596	C1 - C2	0.01904	7.91	1.89	0.94	0.04
			C1 - N10	0.18809	17.32	4.14	0.54	0.04
σ -σ*	N10 - N11	1.98467	C1 - C2	0.01904	14.43	3.45	1.27	0.06
			C13 - S14	0.01241	9.62	2.3	1.17	0.05
σ -σ*	N11 - H12	1.98721	C13 - N15	0.04985	15.52	3.71	1.15	0.06
σ -σ*	N11 - C13	1.98836	C1 - N10	0.01912	7.57	1.81	1.46	0.05
			N15 - H16	0.00802	9.25	2.21	1.27	0.05
σ -σ*	C13 - S14	1.98217	C13 - S14	0.49924	24.39	5.83	0.21	0.04
π -σ*	C13 - S14	1.9764	N10 - N11	0.03491	19.16	4.58	1.05	0.06
			C13 - N15	0.04985	4.48	1.07	1.16	0.03
			N15 - H17	0.01951	13.31	3.18	1.1	0.05
σ -σ*	C13 - N15	1.99177	N11 - H12	0.03538	9.96	2.38	1.24	0.05
σ -σ*	N15 - H16	1.98839	N11 - C13	0.0586	18.41	4.4	1.1	0.06
σ -σ*	N15 - H17	1.98528	N11 - C13	0.0586	4.39	1.05	1.11	0.03
			C13 - S14	0.01241	23.1	5.52	0.98	0.07
n -σ*	LP N10	1.91979	C1 - C2	0.01904	7.49	1.79	0.81	0.03
			C1 - C6	0.03486	46.74	11.17	0.79	0.09
n -σ*	LP N10	1.91979	N11 - H12	0.03538	38.53	9.21	0.77	0.08
			N15 - H17	0.01951	6.61	1.58	0.81	0.03
n -π*	LP N11	1.66979	C1 - N10	0.18809	114.1	27.27	0.29	0.08
			C13 - S14	0.49924	273.93	65.47	0.22	0.11
n -σ*	LP S14	1.98468	N11 - C13	0.0586	11.3	2.7	1.12	0.05
			C13 - N15	0.04985	15.27	3.65	1.16	0.06
n -σ*	LP S14	1.88099	N11 - C13	0.0586	47.2	11.28	0.62	0.08
			C13 - N15	0.04985	48.87	11.68	0.66	0.08
n -σ*	LP N15	1.71823	C13 - S14	0.49924	320.83	76.68	0.21	0.12

Table 7: NBO analytical data of Acetone Thiosemicarbazone.

T (K)	S_m^0 (cal mol^{-1} K^{-1})	$C_{p,m}^0$ (cal mol^{-1} K^{-1})	ΔH_m^0 (kcal mol^{-1})	Gibbs free energy $\Delta G = \Delta H - T\Delta S$ KJmol^{-1}
100	318.20	120.76	7.20	-31812.8
200	428.65	204.68	23.61	-85706.4
298.15	**523.81**	**275.66**	**47.24**	**-15612.7**
300	525.52	276.95	47.75	-157608.0
400	614.41	342.99	78.81	-245685.0
500	697.29	400.34	116.05	-348529.0
600	774.65	448.33	158.56	-464631.0
700	846.86	488.37	205.45	-592597.0
800	914.34	522.18	256.03	-731216.0
900	977.56	551.08	309.73	-879494.0
1000	1036.94	576.00	366.11	-1036574.0

Table 8: Thermodynamic properties at different temperatures.

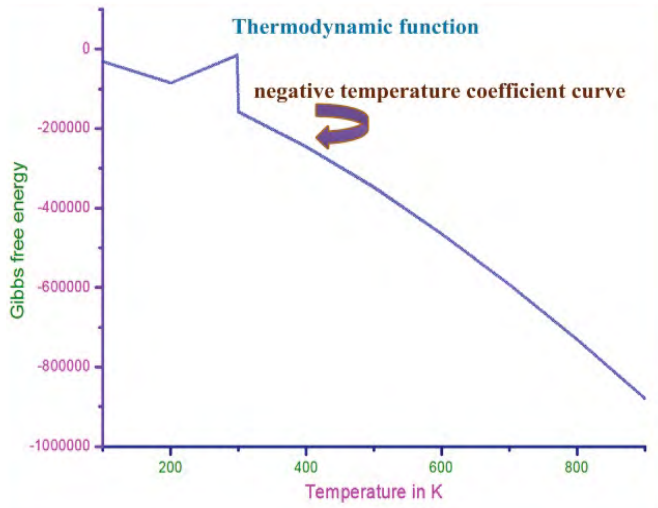

Figure 10: Thermodynamic variation diagram of Acetone Thiosemicarbazone.

Parameters	Values		
HOMO	-8.24218 eV		
LUMO	-4.69835 eV		
Energy gap	3.54383 eV		
Ionization potential (IP)	-8.24218 eV		
Electron affinity (EA)	-4.69835 eV		
Electrophilicity Index (ω)	11.812		
Chemical Potential (μ)	6.470		
Electronegativity (χ)	-6.470 eV		
Hardness (η)	-1.772		
Softness (S)	0.2822		
Dipole moment (Debye)	5.713 Debye		
Parameters	**Thiosemicarbazide (A)**	**Acetone (B)**	**Electrophilicity charge transfer (ECT) $(\Delta N_{max})_A$-$(\Delta N_{max})_B$**
Chemical Potential (μ)	6.012	3.82	+0.47
Chemical Hardness (η)	-3.438	-2.99	
ΔN_{max}= -μ/ η	1.75	1.28	

Table 9: Chemical parameters of Acetone thiosemicarbazone.

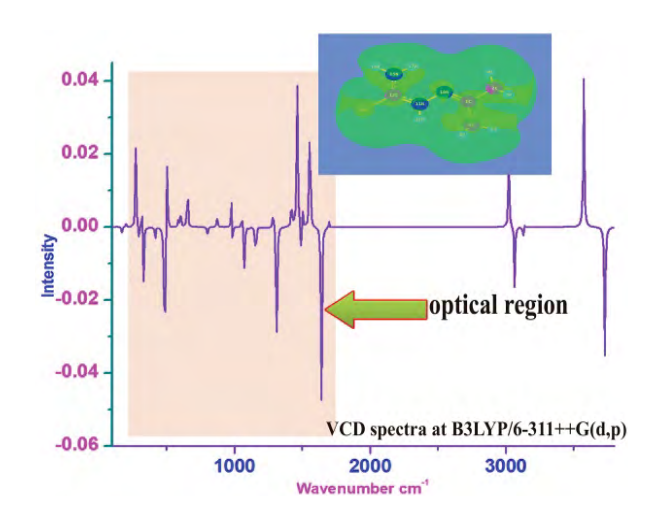

Figure 11: VCD spectra of Acetone Thiosemicarbazone.

Electrophilicity index is a factor which is used to measure the energy lowering due to maximal electron flow between ionization potential and electron affinity. The Electrophilicity index was 11.81 and was high which ensured the energy transition between donor (HOMO) and acceptor (LUMO). This was inferred that, the band gap of the present compound was within the limit and exhibit the semiconducting nature. The electrophilicity based charge transfer (ECT) is another important physico chemical function which provides the exchange of energy and charges from base to functional group of vice versa. If ECT is greater than zero, the charges will be moved from base to functional group. If ECT is less than zero, the charges will be tending to move from functional group to base compound. In this case, the base and functional group were thiosemicarbazone and was acetone respectively. The ECT was +0.47 which was greater than zero. So, here, the charges moved from acetone to thiosemicarbazone to persuade the NLO property.

VCD analysis: Vibrational circular dichroism (VCD) is electro-optic effect which exhibits vibrational optical activity of IR form and detects differences in attenuation of left and right circularly polarized light passing through the compound. It is the extension of circular dichroism spectroscopy into the IR and near infrared region. The VCD provides two-dimensional vibrational structural information since VCD is sensitive to the mutual orientation of base and ligand groups in a molecule. It is also used for the identification of absolute configurations of the organic compounds. The result of a VCD measurement is the combination of emission and absorption spectra, figure out the elucidation of chemically and optically significant molecules.

The VCD spectrum and (Mirror reflection) enantiomers of the present compound was portrayed in Figure 11. In this present case, though, the spectrum was initiated from zero, the rigorous signals were appeared in mid infrared region and the intensity of the absorption and emission were elevated in positive and negative dimensions due to the left and right circular polarization. The absorption intensity is usually unequal on both sides (up and down) of the VCD spectrum, in this case, the probability of incorporation was found to be higher in absorption side than emission. This was mainly due to the C=N, C=S, C-C, N-N, N-H and C-N stretching vibrations. There were two additional spectral peaks observed for N-N and C-H stretching. In the present case, the optical second and third order dichroism was effective and this circumstance was optimistic to the temptation of the NLO properties.

Conclusion

The geometry of the present molecule was optimized in HF and DFT level of theories and the optimized parameters have been calculated and presented. The alternation of the bonds and bond angles with respect to methyl groups are discussed. The Mulliken charge analysis has been carried out in order to explain the redistribution of charges and simultaneously, the change of physical and chemical properties are interpreted. From the observation, it was clear that, the molecule is very reactive for electrical and optical properties. As this compound optically active, the addition of acetone group was further improving the electronic and optical activity. The vibrational sequence of the molecular bonds corresponding to the region of IR and Raman regions are studied in detail. From the NMR chemical examination, it is very important to note that, the introduction of acetone groups as new substituent in a compound was increased the crystal efficiency in moderate way. From the optical results, it is observed that, the molecular Polarizability and hyperpolarizability are dynamic. So, the present compound can be used to prepare NLO crystals. From the

NBO analysis of the present compound, it is believed that, most of the interactions are taking place between BD to BD* and BD to RY*. Thus, by the electron cloud transformation, the charge distribution is customized according to the orbital interaction.

References

1. Shi Y, Zhang C, Bechtel JH, Dalton LR, Robinson BH, et al. (2000) Low (Sub-1-Volt) Halfwave Voltage Polymeric Electro-optic Modulators Achieved by Controlling Chromophore Shape. Science 288: 119-122.
2. Kajzar F, Lee KS, Jen AKY (2003) Advanced Polymer Science 161: 1.
3. Krishnakumar V, Nagalakshmi R (2008) Studies on the first-order hyperpolarizability and terahertz generation in 3-nitroaniline. Physica B 403: 1863-1869.
4. Millefiori S, Alparone A (2000) Second hyperpolarisability of furan homologues C4H4X (X=O, S, Se, Te): ab initio HF and DFT study. Chemical Physics Letters 332: 175-180.
5. Kamada K, Ueda M, Nagao H, Tawa K, Sugino T, et al. (2000) Molecular Design for Organic Nonlinear Optics: Polarizability and Hyperpolarizabilities of Furan Homologues Investigated by Ab Initio Molecular Orbital Method. Journal of Physical Chemistry A 104: 4723-4734.
6. Mishra SR, Rawat HS, Laghate MM (1998) Nonlinear absorption and optical limiting IN metalloporphyrins. Nonlinear and Optical Communication 147: 328-332.
7. Nalwa, Miyata HS (1997) Nonlinear Optics of Organic Molecules and Polymers. CRC Press, Boca Raton, FL.
8. Sutherland RL (1996) Handbook of Nonlinear Optics. Marcel Dekker, New York, USA.
9. Indrani P, Falguni B, Samaresh B (2002) Thiosemicarbazone complexes of the platinum metals. A story of variable coordination modes. Indian Academic Sciences 4: 255-268.
10. Savithiri S, Arockia doss M, Rajarajan G, Thanikachalam V, Bharanidharan S, et al. (2015) Spectroscopic (FT-IR, FT-Raman) and quantum mechanical studies of 3t-pentyl-2r,6c-diphenylpiperidin-4-one thiosemicarbazone. Spectrochim Acta A Mol Biomol Spectrosc 136 Pt B: 782-792.
11. Anoop MR, Binil PS, Suma S, Sudarsanakumar MR, Sheena M, et al. (2010) Vibrational spectroscopic studies and computational study of ethyl methyl ketone thiosemicarbazone. Journal of Molecular Structure 969: 48-54.
12. Yusuf S, Barbara M, Cagri C, Hatice D, Daniel S, et al. (2014) Vibrational spectroscopy (FT-IR and Laser-Raman) investigation, and computational (M06-2X and B3LYP) analysis on the structure of 4-(3-fluorophenyl)-1-(propan-2-ylidene)-thiosemicarbazone. Spectrochimica Acta Part A: Molecular and Biomolecular Spectroscopy 128: 91-99.
13. Hernándeza W, Paz J, Vaisberg A, Spodine E, Richter R, et al. (2008) Synthesis, characterization, and in vitro cytotoxic activities of benzaldehyde thiosemicarbazone derivatives and their palladium (II) and platinum (II) complexes against various human tumor cell lines. Bioinorg Chem Appl.
14. Santhakumari R, Ramamurthi K (2011) Structural, thermal and optical characterization of an organic NLO material--benzaldehyde thiosemicarbazone monohydrate single crystals. Spectrochim Acta A Mol Biomol Spectrosc 78: 653-659.
15. Frisch MJ (2010) Gaussian 09, Revision D.01, Gaussian, Inc., Wallingford, CT, USA.
16. Lee C, Yang W, Parr RG (1988) Development of the Colle-Salvetti correlation-energy formula into a functional of the electron density. Phys Rev B Condens Matter 37: 785-789.
17. Frisch MJ, Nielsm AB, Holder AJ (2010) Gaussview User Manual, Gaussian, Pittsburgh, USA.
18. Hubert JI, Kostova I, Ravi Kumar C, Amalanathan M, Pinzaru SC (2009) Theoretical and vibrational spectral investigation of sodium salt of acenocoumarol. Journal of Raman Spectroscopy 40: 1033-1038.
19. Ledesma AE, Zinczuk J, Ben AA, Lopez Gonzalez JJ, Brandan SA, et al. (2009) Synthesis and vibrational analysis of N-(2′-Furyl)-Imidazole. Spectrosc 40: 1004-1010.
20. Per Lind (2007) Organic and Organometallic Compounds for Nonlinear Absorption of Light. Umea University, Sweden.
21. Kalsi PS (2009) Spectroscopy of Organic Compounds. New Age International (P) Limited, Publishers.
22. Krishnakumar V, Balachandran V (2005) DFT studies, vibrational spectra and conformational stability of 4-hydroxy-3-methylacetophenone and 4-hydroxy-3-methoxyacetophenone. Spectrochim Acta A Mol Biomol Spectrosc 61: 2510-2525.
23. Rumi M, Zerbi G (1999) Conformational dependence of vibrational and molecular nonlinear optical properties in substituted benzenes: the role of π-electron conjugation and back-donation. Journal of Molecular Structure 509: 11-28.
24. Sundaraganesan N, Priya M, Meganathan C, Joshua BD, Cornard JP (2008) FT-IR, FT-Raman spectra and quantum chemical calculations of 3,4-dimethoxyaniline. Spectrochim Acta A Mol Biomol Spectrosc 70: 50-59.
25. Green JHS, Harrison DJ, Kynoston W (1971) Vibrational spectra of benzene derivatives-XII 1,2,4-trisubstituted compounds. Spectrochimica Acta 27A: 807-810.
26. Roeges NPG (1994) A Guide to the Complete Interpretation of Infrared Spectra of Organic Structures. Wiley, New York, USA.
27. Schettino V, Sbrana G, Righini R (1972) Evidence for a phase transition in crystalline pyrazine. Chem Phys Lett 13: 284-285.
28. Altun A, Golcuk K, Kumru M (2003) Theoretical and experimental studies of the vibrational spectra of m-methylaniline. Journal of Molecular structure 625: 17-24.
29. Durig JR, Bergana MM, Phan HV (1991) Raman and infrared spectra, conformational stability, barriers to internal rotation, ab initio calculations and vibrational assignment of dichloroacetyl fluoride. Journal of Raman spectroscopy 22: 141-146.
30. Gunasekaran S, Varadhan SR, Manoharan K (1993) Asian J Phys 2: 165-172.
31. Tsuboi M (1960) ^{15}N isotope effects on the vibrational frequencies of aniline and assignments of the frequencies of its NH_2 group Spectrochimica Acta Part A 16: 505-512.
32. Ohno K, Yoshitaka M, Hiroatsu M (1992) Vibrational spectra and molecular conformation of taurine and its related compounds. Molecular Structure 268: 41-50.
33. Singh RN, Kumar A, Tiwari RK, Rawat P, Verma D, et al. (2012) Synthesis, molecular structure and spectral analysis of ethyl 4-formyl-3,5-dimethyl-1H-pyrrole-2-carboxylate thiosemicarbazone: A combined DFT and AIM approach. Journal of Molecular Structure 1016: 97-108.
34. Boobalan MS, Ramalingam S, Amaladasan M, Tamilvendan D, Venkatesa Prabhu G, et al. (2014) A computational perspective on equilibrium geometry, vibrational spectra and electronic structure of antioxidant active Mannich base 1-[(Pyridin-2-yl amino) methyl] pyrrolidine-2,5-dione. Journal of Molecular Structure 1072: 153-172.
35. Silverstein RM, Webster FX (2005) Spectroscopic Identification of Organic Compounds. 7th edn. Wiley, New York, USA.
36. Sundaraganesan N, Karpagam J, Sebastian S, Cornard JP (2009) The spectroscopic (FTIR, FT-IR gas phase and FT-Raman), first order hyperpolarizabilities, NMR analysis of 2,4-dichloroaniline by ab initio HF and density functional methods. Spectrochim Acta A Mol Biomol Spectrosc 73: 11-19.
37. Shunmugam R, Sathyanarayana DN (1984) Spectrochimica Acta Part A 41: 757-761.
38. Anbarasan R, Dhandapani A, Manivarman S, Subashchandrabose S, Saleem H (2015) Synthesis and spectroscopical study of rhodanine derivative using DFT approaches. Spectrochim Acta A Mol Biomol Spectrosc 146: 261-272.
39. Ahuja S (1998) Impurities Evaluation of Pharmaceuticals. Marcel Dekker, New York, USA. pp: 142-144.
40. Jean, Yvesand, Volatron, Francois (2005) An Introduction to Molecular Orbitals. Oxford University Press.
41. Housecroft, Catherine, Sharpe, Alan (2007) Inorganic chemistry. 3rd edn, Prentice Hall.
42. Mohan J (2004) Organic spectroscopy: Principles and Applications. Narosa publishing House, New Delhi.
43. Balc M (2005) Basic p1 sH and p13 s CNMR spectroscopy. 1st edn. Elsevier, Amsterdam 12: 427.

44. Ramalingam S, John David EI, Ramachandra Raja C, Jobe Prabakar PC (2014) Spectroscopic [IR and Raman] Analysis and Gaussian Hybrid Computational Investigation- NMR, UV-Visible, MEP Maps and Kubo Gap on 2,4,6-Nitrophenol. J Theor Comput Sci 1: 2.

45. Dukor RK, Nafie LA (2000) In Encyclopedia of Analytical Chemistry: Instrumentation and Applications. Eds Meyers RA (Wiley, Chichester, UK). pp: 662-676.

46. Keiderling TA, Xu Q (2002) Unfolded peptides and proteins studied with infrared absorption and vibrational circular dichroism spectra. Adv Protein Chem 62: 111-161.